White-Light Coronal Imaging at the 21 August 2017 Total Solar Eclipse

Jay M. Pasachoff[1] (ID) **· Vojtech Rušin[2]** (ID)

Abstract

We describe the solar corona as imaged in the 21 August 2017 total solar eclipse from sites in Oregon and Illinois, USA separated by nearly one hour. Our composite images, each made from dozens of individual frames, show helmet streamers, nearly radially oriented narrow rays, and polar coronal holes filled with polar plumes. The Ludendorff flattening index of 0.24 is compared with measurements from the last two centuries. We discuss the most remarkable coronal dynamics detected over a nearly one-hour interval between the two observing sites.

Keywords Eclipses · Sun · Magnetic fields, corona · Structures and dynamics

1. Introduction

Observations of the white-light solar corona during a total solar eclipse are rare, occurring $\approx 74-75$ times every 100 years, give or take a few days of bad weather. They provide an irreplaceable occasion to observe the great variability in coronal structure, from large coronal holes and helmet streamers to small-scale structures of only 1 arcseconds, (e.g. November and Koutchmy, 1996; Koutchmy, 1988; Habbal et al., 2021), from coronal-mass-ejection (CME) and polar-plume dynamics to the continuous flow of particles of different velocities in the solar wind (e.g. Pasachoff et al., 2008; Filippov, Koutchmy, and Lefaudeux, 2020 and references therein; Boe, Habbal, and Druckmüller, 2020). The "Great American Eclipse" of 21 August 2017 provided an unusual opportunity to observe the coronal structure, which is formed by the magnetic fields of the Sun via global and local fields (Golub and Pasachoff, 2010, 2017; Pasachoff, 2017a,b, 2018).

We provide analysis of the composite images from the multiple photographic images obtained by our team during totality on 21 August 2017, elaborating on the discussion of Pasachoff et al. (2018). We are interested in the shape and structure of the white-light corona

✉ J.M. Pasachoff
eclipse@williams.edu

V. Rušin
vrusin@ta3.sk

[1] Williams College – Hopkins Observatory, Williamstown, MA 01267, USA

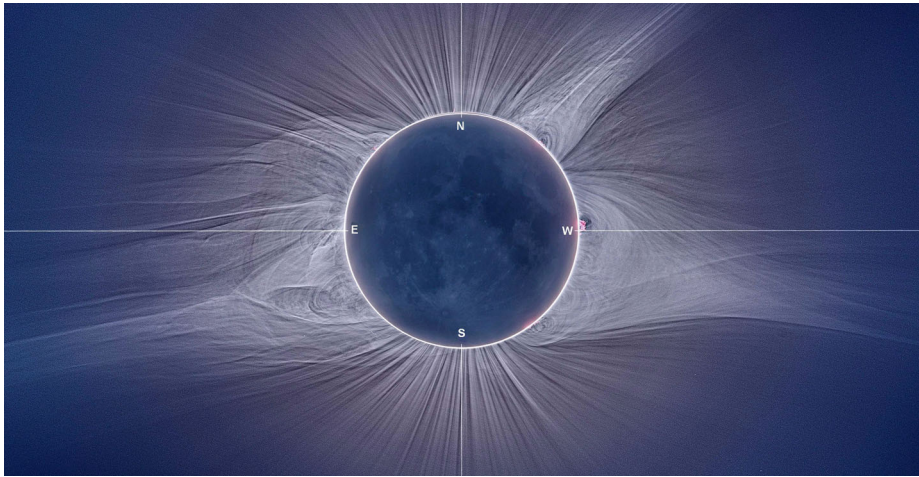[2] Astronomical Institute, Slovak Academy of Sciences, 059 60 Tatranská Lomnica, Slovakia

Figure 1 The white-light corona (WLC) was imaged for an interval centered at 17:18 UTC 21 August 2017 by the Williams College Eclipse Expedition at Salem, Oregon, USA, with an 800 mm Nikkor telephoto lens on a Nikon D810 and processed by R. Vaňúr.

(WLC), the temporal structure changes over one hour, and the ellipticity as an indicator of a long-term parameter for solar magnetic fields.

We were positioned to observe the eclipse soon after the path of totality (about 130 km in width) reached the west coast of the United States.

The Williams College Eclipse Expedition was positioned on a terrace of the computer-science building at Willamette University in Salem, Oregon, USA at 44° 56′ 07.6″ N, 123° 01′ 54.4″ W. The total solar eclipse occurred in ideal weather conditions starting at 17:17:20 UTC (10:17:20 Pacific Daylight Time) and lasted 1 minute 54.8 seconds; 1 minute 53.0 seconds as calculated to consider limb corrections. Figure 1 shows the final composite image, processed by R. Vaňúr, which was composed of 85 images of different exposures from 0.001 – 1 second, using an 800 mm Nikkor telephoto lens and a Nikon camera. Figure 2 shows the WLC as obtained at Carbondale, Illinois, USA by the Economou group 64 minutes later. We make our dynamic analyses of the coronal structures from these two observations.

The Salem data will be used for general analysis, while the Carbondale data will only be used for analyzing notable dynamic changes in various coronal structures. It is worth noting that the Carbondale data are of a slightly lower quality (e.g. in spatial resolution) than those from Salem.

2. Analysis

The eclipse took place about two years before the minimum between Solar Cycles 24 and 25. Solar Cycle 24 was a relatively low-amplitude cycle compared with the previous seven cycles. Two large, bright active areas (see Figures 3, 5, and 6) with sunspot groups appeared on the disc, just North of the solar Equator. One of them, very active, was located above the eastern part of the disc. The second one was located near the central meridian. Both of these groups are associated with strong gradients of the magnetic field as seen in the photospheric magnetic-field map (Figure 3) from the Wilcox Solar Observatory. Dark lines indicate the

Figure 2 The WLC image was obtained by the Economou group at Carbondale, Illinois, USA, with images taken centered at 18:22 UTC 21 August 2017, some 64 minutes after images were taken at our site in Salem, Oregon; processed by R. Vaňúr.
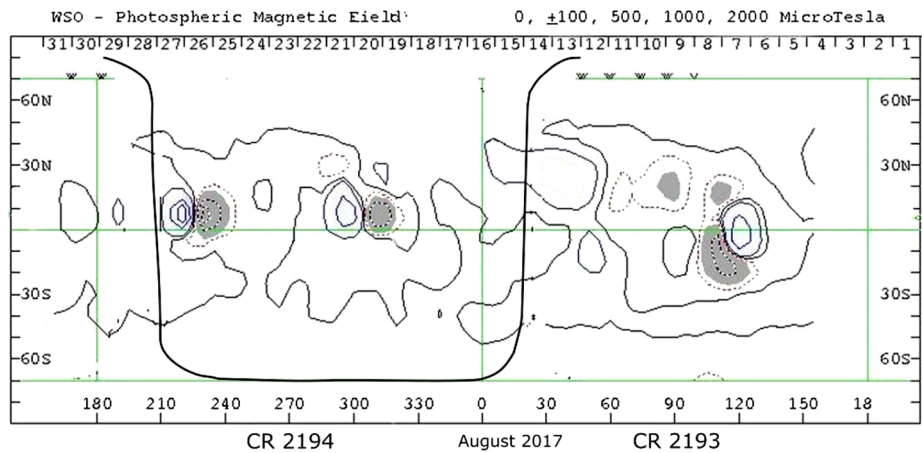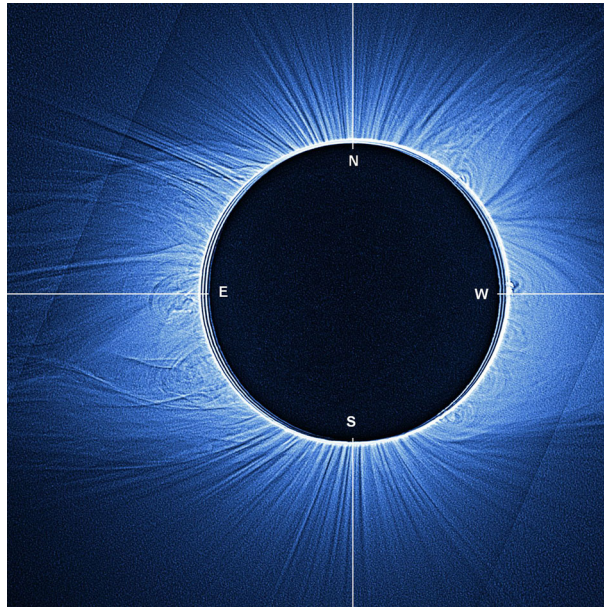

Figure 3 The photospheric magnetic-field chart 2194/2193 for 21 August 2017 and the solar limb outline. Based on the ground-based WSO magnetic-field maps (wso.stanford.edu).

positions of neutral lines observed on the solar surface. Figure 4 shows a composite image of the extrapolated magnetic-field lines and the Salem WLC.

3. Large-Scale Coronal Structures

Helmet streamers and coronal holes are large-scale coronal structures. To investigate them with ground-based and space observations, we combine our corona image with the Naval Research Laboratory's image from the *Large Angle and Spectrometric Coronagraph*-C2
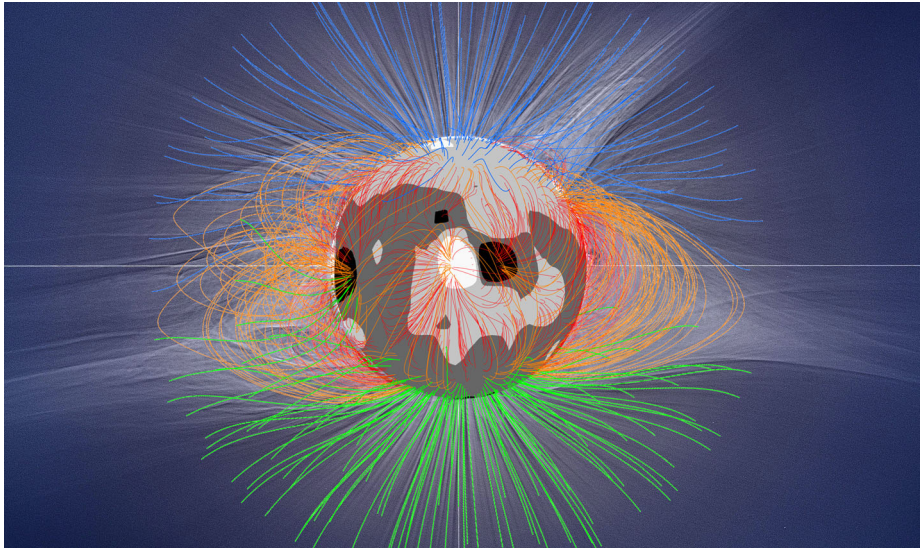
Figure 4 Composite image of extrapolated magnetic-field lines. (Courtesy of Yi-Ming Wang, US Naval Research Laboratory) with the white-light corona observed by our team in Salem, Oregon, USA. North is up.

Figure 5 Combined image of a GOES-16's SUVI filtergram at 30.4 nm, two highly processed images of the inner corona obtained in Salem, and a LASCO-C2 image of the outer corona, all of the 21 August 2017 eclipse. North is up. A, B, and C indicate the brightest streamers in the Salem and LASCO corona. Bright prominences are located on the bases of the B, D, C streamers. Less-pronounced streamers/rays and some polar plumes with lower brightness are marked by *green arrows*.
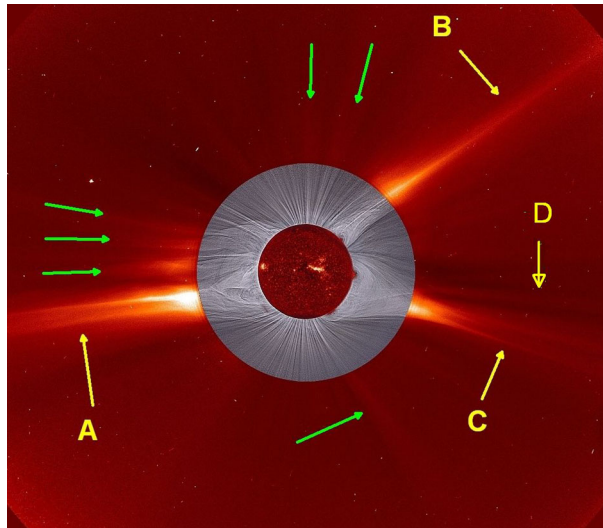
coronagraph onboard ESA's *Solar and Heliospheric Observatory* (SOHO), and the NOAA's GOES-16 *Solar Ultraviolet Imager* (SUVI) image at He ɪɪ 30.4 nm, as seen in Figure 5. In this combined image, we mark two very bright helmet streamers above the solar west limb as A and B and one above the southeast limb as C. Streamer D compared to streamer C appears to be less bright in the part of the SOHO/C2 image indicated by the yellow arrow, but in eclipse images above the surface of the Sun their brightness is nearly identical (see Figures 1 or 2).

Figure 6 The SUVI 19.5 nm corona taken at 23:19:28 UTC, where the northern coronal hole is seen. (Courtesy of D.B. Seaton, Univ. of Colorado, Boulder, and SwRI.) North is up.
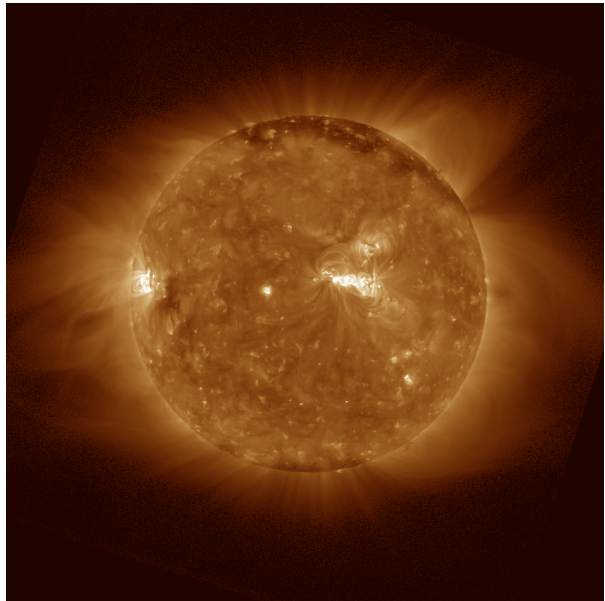
It is expected that three distinctive helmet streamers should be associated with their structure in the lowest corona. In this case, a quiescent prominence surrounded by a coronal cavity is located at the streamer base above the lunar limb. Higher up, concentric loops exist that, due to the solar wind, are elongated to tips that extend outward. The legs of a classic helmet streamer that develops over an active region are anchored in the opposite polarities of the Sun's magnetic field (Wang, Sheeley, and Rich, 2007). The situation in our case, however, appears to be slightly different from that of the classic case. This could be caused by the projection of the observed coronal structures along the line-of-sight. In any case, we conclude that our case is a little more complicated than originally modeled, since the helmet streamers are not entirely related to the Sun's active regions. Let us now look in more detail at the WLC shape obtained from the eclipse.

3.1. Coronal Holes

The coronal shape revealed at this eclipse, as seen in Figures 1, 2, 4, and 6, possessed coronal holes at high latitudes, filled with many polar plumes. The northern coronal hole, seen at first glance in the processed WLC in Figures 1 or 2, is located at position angles (PA) $33 - 338°$, while the southern hole is at PA $151 - 201°$. However, if we assume that the helmet streamer B is located above the isolated magnetic region in the unipolar region of the magnetic field around the North Pole of the Sun (see Figure 5), the northern coronal hole ends around PA $297°$. This confirms the corona seen in SUVI 19.5 nm (Figure 6) and *Solar Dynamics Observatory* (SDO)/*Atmospheric Imaging Assembly* (AIA) 211 Å EUV. On the other hand, the isophotes of the WLC (see Figure 9) do not confirm this. This difference can be explained by the fact that the innermost isophotes of the WLC were obtained at a time when the Moon obscured more of the eastern than the western surface of the Sun.
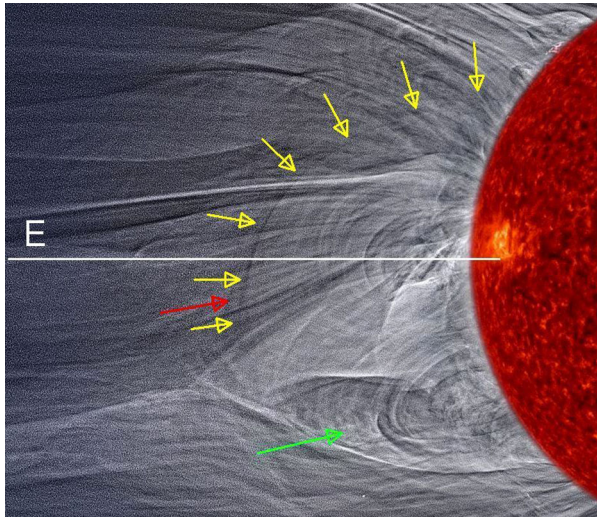
Figure 7 A base of the helmet streamer A above the eastern limb combined with the SUVI 30.4 nm image (Active Region 2472 – a bright area on the solar surface – is located around 5° above the solar Equator). The *green arrow* indicates one loop system (southern); the *red arrow* indicates another system (closer to the Equator). We also mark a black arc (loop) with *yellow arrows* extended very high above the solar limb; it could connect very distant magnetic regions in the photosphere. It could be assumed that this dark arc is part of the bright arcs / loops that lies beneath them. The North Pole is up. (The SUVI 30.4 nm image is courtesy of D.B. Seaton, Univ. of Colorado, Boulder and SwRI.)

3.2. Helmet Streamers

The A helmet streamer is located near PA 103°, as shown in the SOHO/LASCO images in Figures 5 and 7. There are indications of two or three coronal loop systems in its base, an effect of the streamer belt being slightly curved in the line-of-sight. The helmet streamer extends from PA 72 – 145° in the Salem image. If we assume that the loop system marked by the green arrow is located at the base of each helmet streamer, then the helmet streamer that is closer to the South Pole should have its base extend from PA 85 – 145°. The base of the second helmet streamer, which is closer to the Equator, and could be connected to the Active Region 2472 located near the eastern limb, was unidentifiable. It is possible that its northern boundary could be at PA ≈ 70°. There is no prominence at the base of one of the streamers. We did not succeed in linking the A helmet streamer with any specific active area on the solar photosphere or chromosphere.

The A streamer's boundary, above the east limb, is very complex. Figure 7 reveals several threadlike streamers and rays, a number of which are very significant in their brightness and in the continuation of their tips, as marked by green arrows in Figure 5. Several small prominence knots can be found within PA 40 – 59°. There are also some outstanding faint curved rays that are difficult to identify with other coronal structures.

The B streamer is located within PA 303 – 335°, with its position on the SOHO image centered at PA 312°. Two small prominences are at its base at PA 312° and 326°, respectively. They are surrounded by small coronal cavities and loops, which continue to the pointed tip high above the solar surface. This creates a very clear threadlike streamer that dominates the helmet streamer. Details of the bottom part of the streamer are shown in Figure 8. A detailed view of this helmet streamer displays its complicated inner structure,

Figure 8 Detail of B helmet streamer with its interior loops and thin rays; the North Pole is up.
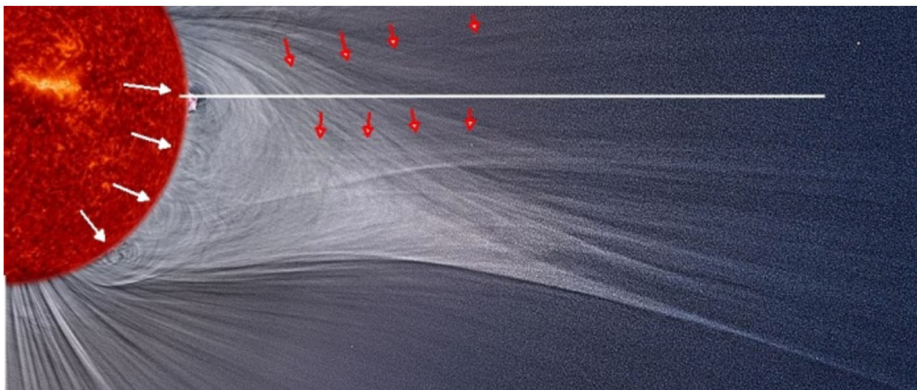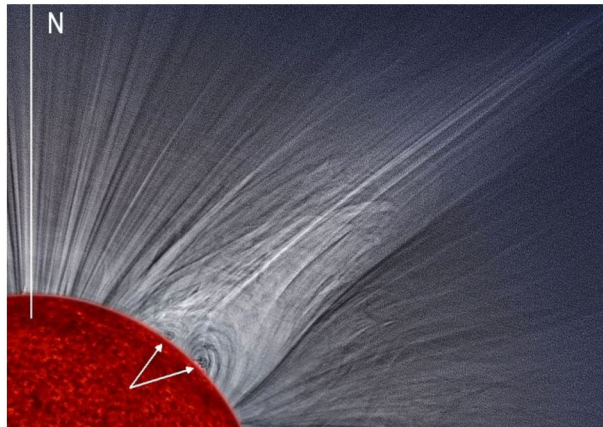

Figure 9 Detail of the streamer base (marked by the letters C and D in Figure 5) above the southwest limb. The white line shows the westward direction. The four loop systems above the solar limb are denoted by *white arrows*. The *red arrows* show two very interesting alternating dark–bright quasi-vertical streaks or threads. A coronal cavity appears above the bright prominence. North is up.

composed of loops and radially oriented thin rays. At greater heights, the classical coronal loops turn into quite "blurred" formations, reminiscent of the rising output currents of thunderclouds on Earth. In other words, there is additional coronal material mixed with the thin needle-like rays in each structure. The occurrence of the B helmet streamer, or quasi-helmet streamer, as introduced by Wang, Sheeley, and Rich (2007) using the rooting of helmet-streamer legs, was not forecast by the forecasting group at Predictive Science Inc., which forecast other large-scale structures for the 2017 eclipse (Mikić et al., 2018).

The C and D streamers appear above the SW limb, around PA 255° and 264° on the brightest part of the SOHO image. As seen in Figure 1, determining the base of both streamers (furthermore; their separations at higher heights are nicely seen in Figure 9) near the lunar limb within PA 202 – 305° is very complicated if not impossible. We assume that the contours of the helmet streamers, several of which we observe along the line-of-sight, disappear in the light of the coronal loops present there to heights of about two radii above the Sun (see Figure 9).

The bases of four well-developed loop systems shown in Figure 9. Two of them are located above prominences. One prominence, relatively compact and connected with a coronal cavity, is located at PA 270°, while the second, composed of several small knots, is near PA 218°. Measurements of the magnetic-field structure and its physical properties were studied for this coronal cavity using eclipse and non-eclipse observations by Chen et al. (2018, and references therein). We recall that while the brightness of the D helmet streamer in the SOHO image is very weak compared to the helmet streamer C, this comparison does not apply to their brightness at a certain distance/height above the solar limb in the eclipse pictures (see Figure 5).

The hypothetical base of the helmet streamer located above the prominence at PA 270° (just at the west solar limb) seems to extend from PA 235 – 292°. The position of this helmet streamer in the SOHO image is at PA 270°. The northern boundary of the C helmet streamers is impossible to determine. The complexity of this helmet-streamer system is interesting as there were no active limb prominences at the time of observation, and the north streamer's lower-boundary magnetic field was unipolar. The legs of the southern helmet streamer were anchored in opposite polarities. We suggest that this situation could be caused by the superposition and overlapping effects of many helmet streamers along the line-of-sight above the west limb.

4. Ellipticity

The overall change in the shape and brightness of the solar corona from different vantage points was discussed by Rušin (2000) and more recently by Boe, Habbal, and Druckmüller (2020) and Lamy et al. (2021, and references therein). Ludendorff (1934) marked this change as the flattening coefficient, or ellipticity. It is called the "Ludendorff coronal flattening index" or "Ludendorff flattening coefficient" today, and it is written as ε. In short, it is the hypothetical flattening of the solar corona isophote at $2\,R_\odot$, computed from parameters of the straight line (a and b) that is obtained from measured values of flattening for individual isophotes from the lunar limb to the height of $2\,R_\odot$ in the equatorial and polar directions $\pm 22.5°$. Details of this calculation are given by Rušin (2017). The white-light coronal isophotes of the Salem images are shown in Figure 10. They were obtained by combining three images with different exposures to remove the sharp decrease of the corona brightness with height at the $2\,R_\odot$ isophote. The isophotal flattening is shown in Figure 11. Based on their linear variation, we measured a flattening value of $\varepsilon = 0.24$, which is shown in Figure 10 at the given phase of Cycle 24 ($\varphi = 0.789$, computed according to the relation $\varphi = (T - m_1) / (m_2 - m_1)$, where T is the date of the eclipse observation, m_1 is the preceding minimum, and m_2 the subsequent maximum following for the 2017 eclipse.

The Ludendorff flattening index is the result of the distribution of large-scale white-light coronal structures. See also Pishkalo (2011). These include the streamers and coronal holes, so it is related to the extrapolated photospheric magnetic fields, e.g. Kumar, Paul, and Vaidya (2020).

The current Ludendorff flattening index is interesting because the polar magnetic-field strength has nearly doubled in the last 20 years (Svalgaard, Cliver, and Yohsuke, 2005), but when compared with its value over the nearly 170-year history of its measurement, this decrease in the flattening value for the cycle phase of the eclipse does not change.

We note the lack of correlation between the Ludendorff index so far in the current cycle and the timing of the next sunspot cycle (see Figure 12).
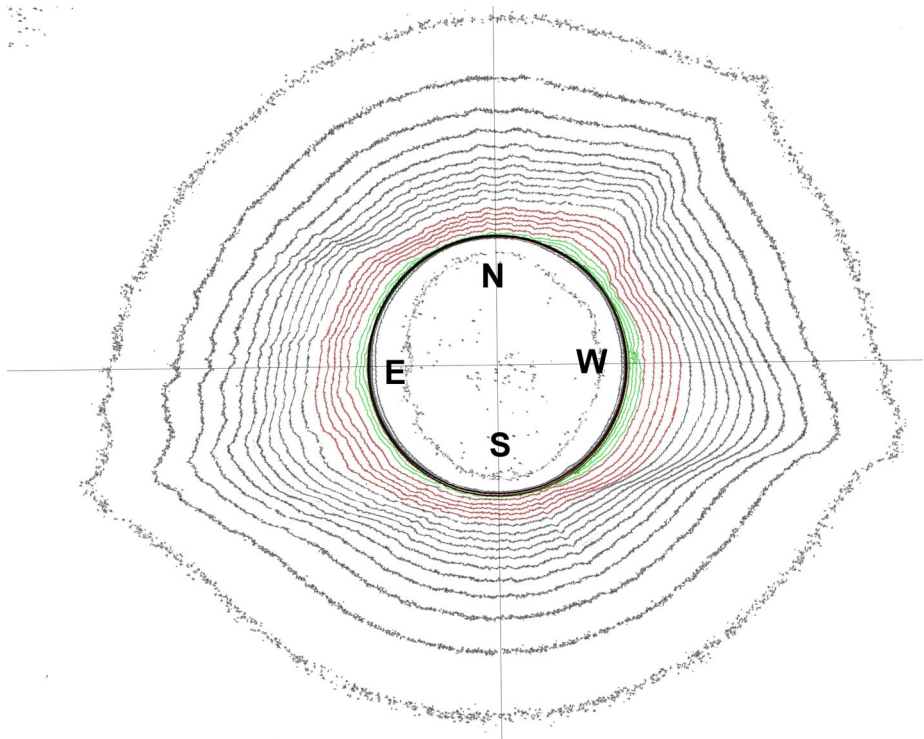
Figure 10 Coronal isophotes as observed up to 3 solar radii (Figure 1) using the Salem corona. Colored isophotes indicate three different exposures: the shortest (1/100 second) one is colored by *green*, middle exposure (1/10 second) in *red*, and 1/2 second as a dark. We note that isophotes are also a very effective means of measuring the radial decrease in corona brightness anywhere around the Sun.

A dispersion in the values shown in Figure 12 at the end of the current solar cycle and the beginning of the new solar-activity cycle could be caused by both changes in the image processing methods over the years and the unexpected occurrence of new helmet streamers. The coronal activity from the old and the new cycles overlaps as the new cycles begin.

5. Coronal Dynamics

Comparing coronal images over the near-one-hour-long span of observed totality from different terrestrial locations sometimes shows large-scale changes, such as the coronal mass ejections that were sometimes observed (e.g. Zirker et al., 1992). Figures 13 left and right show structural coronal changes over the span of just over one hour. The corona in Figure 13 left was obtained in Salem, Oregon, while Figure 13 right was obtained in Carbondale, Illinois. Although the corona in Figure 13 right has slightly lower resolution than that shown in Figure 13 left, some of the observed changes over the 64 minutes are still evident, as identified by yellow arrows. It is difficult to say whether the visible large-scale structural changes are caused by a change in the observational position, although the rotation of the Sun in the hour-long interval between our observing sites is only about half a degree, or are the result of dynamic changes in the corona. We note that there has been no significant change in the loop
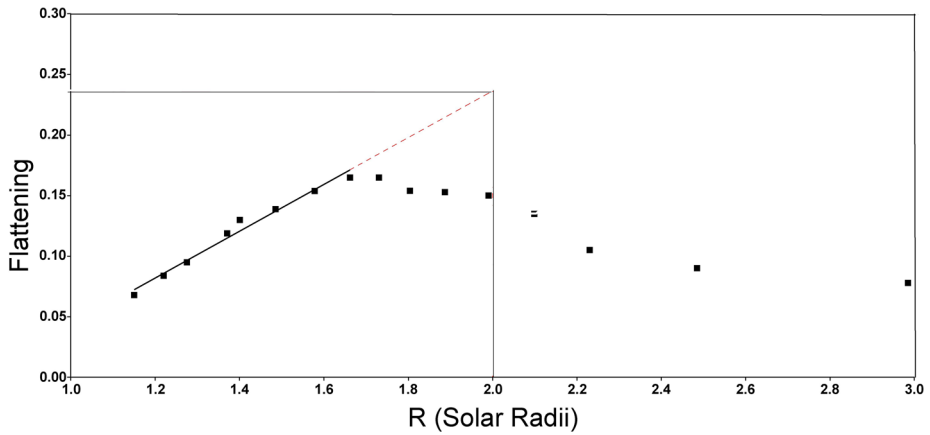
Figure 11 The variations of the ellipticity with the height above the Sun as measured from Figure 8. The computation of the Ludendorff index was from the straight-line fit to the first eight values of individual flattening, matching its definition.
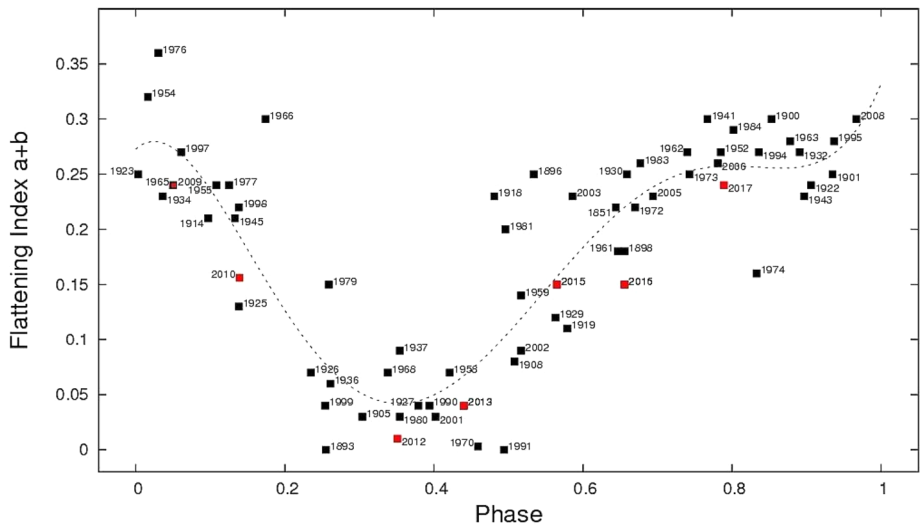

Figure 12 The Ludendorff flattening index over time, as derived from all available eclipses. *Red squares* indicate the flattening index for Cycle 24 only.

system. It would be ideal to have similar observations from other totality sites at different time intervals, although the resolutions of the Megamovie's frames (Peticolas et al., 2019; Hudson et al., 2021) are too low. The green arrow (bottom right) in Figure 13 left indicates a feature that changes in the 64-minute interval from Salem to Carbondale. The yellow arrows at the left of Figure 13 right indicate a part of a dynamic prominence as observed during the eclipse that led to the CME (Filippov, Koutchmy, and Lefaudeux, 2020). This part of the prominence was also observed with SUVI in the 30.4 nm image.

Changes in the brightness of the polar plumes were observed in the coronal hole above the northern pole. We show them in Figure 14 left, from Salem, and 14 right, from Carbondale.
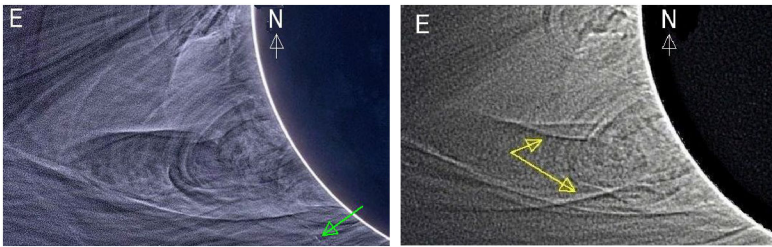
Figure 13 Structural changes at the lower corona in the helmet streamer A, denoted by *yellow arrows*. *Left*: Salem corona, *right*: Carbondale. We thank Thanasis Economou, U. Chicago, for the Carbondale image. The North Pole is up.

The green arrow in Figure 14 left points to the polar plume, which was very bright in Salem but hardly visible in Carbondale, although marked on the image with a yellow arrow. These changes in the brightness of the plumes over the 64-minute interval can only be explained by the fact that in the polar plumes the mass flows from the Sun towards the heliosphere. It is not possible to determine the exact speed because of an uncertainty in the height of the plume, which is determined by its brightness. Based on an approximate estimate of the brightness change in the plume marked with a yellow arrow, we can assume that flows in polar plumes are around 100 km s^{-1}. Speeds from 30 to 100 km s^{-1} were obtained by Bělik et al. (2012) in the 2008 eclipse polar plumes. We note that a slight change in the coronal structure also occurs in the area where there are very small prominences at PA 45°, but the appearance of the prominences is almost identical in images from both sites. Dynamic changes during the eclipse in the north polar region and in the EUV corona were discussed by Hanaoka et al. (2018).

Figure 9 shows two very interesting alternating dark–bright quasi-vertical streaks or threads, denoted by red arrows. The dark line, closer to the bright prominence, is accompanied by a bright coronal ray. We cannot tell if it is a mere projection effect. However, similar narrow streaks and a dark arc above the east limb have been also located in Druckmüller's processed image for this eclipse (www.zam.fme.vutbr.cz/~druck/Eclipse/Ecl2017u/Ma/Mackay_1000mm/00-info.htm).

6. Overall Coronal Structure

If we look in detail at the processed corona, we can see that the white-light corona is made up of small structures, as helmet streamers are not continuously filled with matter in the form of free electrons. In the white-light corona structure, various loop systems, thin radial rays, polar plumes, and discontinuities are observed, as reported by Koutchmy (1988), for example. In our current processing, the smallest structures' images are 4 – 5 arcseconds.

From our point of view, the most interesting feature in these small-scale structures is a huge dark arc or loop, indicated by the red arrow near the A streamer in Figure 7. Interestingly, the arc is at a substantial height above the solar limb at about 0.85 R$_\odot$, almost the top of the loop systems located below it. The footpoints on the Sun are anchored far apart. The left part of the arc is not visible, but if we consider that from the top of its arc to the point where it can still be seen at the limb of the Sun, it reaches a value of PA 51°, then the whole base of the arc extends to a value of about 102°. It is an extremely broad base and cannot be explained by the existence of the helmet streamers that have been observed so far or the localized loop systems in such broad streamers. The dark threads are very close to the
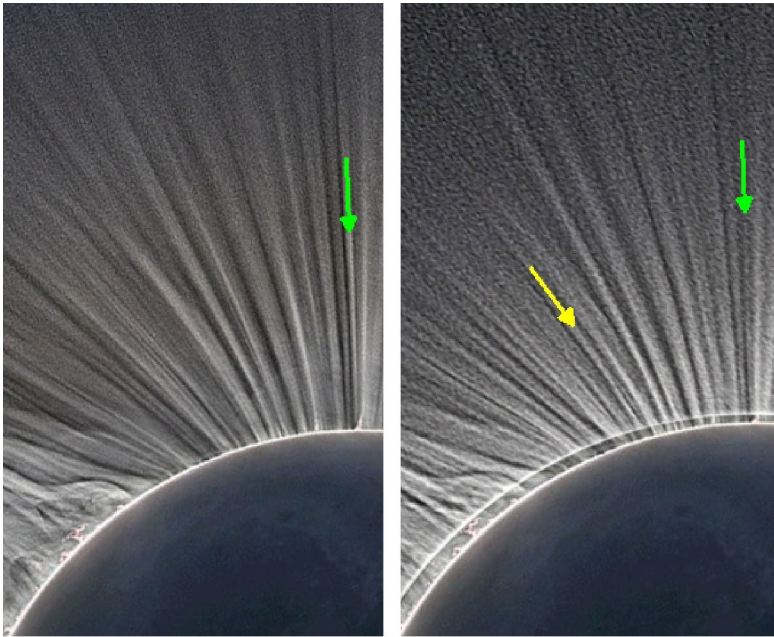
Figure 14   The same area above the northern pole (North up) obtained in Salem, Oregon (*left*), and in Carbondale, Illinois (*right*), just over one hour later. The *green arrow* in both pictures denotes the significant brightness decrease in one polar plume. The *yellow arrow* indicates a "new" polar plume or an old one in its brightness intensification.

solar surface and were observed in 1991 and analyzed by November and Koutchmy (1996). They concluded "the dark threads are fully evacuated", meaning that they are empty of free electrons. This dark arc is not an effect of data processing. It is seen in Druckmüller's image and particularly by Lamy et al. (2021). (For Druckmüller's 2017 images, see www.zam.fme.vutbr.cz/~druck/eclipse/Ecl2017u/0-info.htm.)

A detailed analysis of prominences over the western solar limb gives the impression that the thin coronal rays began to appear out of the fine prominence knots. The first such case was discussed by Koutchmy et al. (1988). We find it interesting that the coronal rays could seem to come from the prominences. We cannot at this point determine if it is a real effect or a projection effect.

General eclipse links for educational purposes are summarized in Pasachoff and Fraknoi (2017). For other 2017-eclipse analysis, see Bemporad (2020), Caspi et al. (2019), Judge et al. (2019), Liang et al. (2021), Madsen et al. (2019a), Samra et al. (2018), and Williams et al. (2020). For earlier-eclipses' imaging of coronal structure, see, for example, Druckmüller et al. (2006), Pasachoff et al. (2007, 2011a,b, 2015, 2022), and Zirker et al. (1992). For early analysis of the 2019 eclipse corona, see Madsen et al. (2019b), Pasachoff et al. (2020). For continued disk imaging in the EUV with SUVI on GOES spacecraft, see Seaton et al. (2020).

7. Conclusions

We have analyzed our photographic observations of the eclipse of 21 August 2017. The major sunspot group of that day was too close to the disk center to affect limb structures.

Based on our analysis, we came to the following conclusions:

i) The coronal shape showed several streamers; two coronal holes with polar plumes were also seen.

ii) The Ludendorff flattening index $[\varepsilon = a + b]$ reached a value of 0.24, which we compare with many historic values for this phase about three-quarters of the way through the activity cycle.

iii) Over a near-hour-long interval between sites, we observed changes in a streamer's base and in polar plumes, perhaps showing coronal material turning into the solar wind. These can be compared with Hanaoka et al. (2018), who identified six jets over a similar time interval. The observed EUV and X-ray jets were apparently connected. We observed a southeast dark arc with feet over 100° apart.

iv) We identified two rare alternating dark–bright streaks above the west limb. See Figure 9.

v) We imaged some thin coronal rays or loops above the prominences.

8. General Remarks

We studied the structure of the dynamic corona at a variety of spatial scales. We look forward to being able to observe the coronal magnetic field with the *Daniel K. Inouye Solar Telescope* and comparing it with visible imaging at future eclipses. Changes in the coronal shape and structure can be caused by visible features, e.g. CMEs, dynamics of prominences, extreme ultraviolet waves, jets, or by "stealth CMEs" as discussed recently by Alzate and Morgan (2017). Habbal's Solar Wind Sherpas group (Boe et al., 2020) show changes resulting from a CME from three sites during the 2017 eclipse separated by 28 minutes (1400 km along the path).

We provide an alternative analysis of WLC images of the 2017 eclipse to that of Filippov, Koutchmy, and Lefaudeux (2020), linking with comments from our group about the shape of the corona observed by Lefaudeux at extremely high resolution during the 2019 eclipse (Lockwood et al., 2020).

Declarations

References

Alzate, N., Morgan, H.: 2017, Identification of low coronal sources of "stealth" coronal mass ejections using new image processing techniques. *Astrophys. J.* **840**, 103.

Bělik, M., Rušin, V., Saniga, M., Barczynski, K.: 2012, Dynamics of polar plumes during the total solar eclipse of August 1, 2008. *Contrib. Astron. Obs. Skaln. Pleso* **42**, 125.

Bemporad, A.: 2020, Coronal electron densities derived with images acquired during the 2017 August 21 total solar eclipse. *Astrophys. J.* **904**, 178. DOI.

Boe, B., Habbal, S., Druckmüller, M.: 2020, Coronal magnetic field topology from total solar eclipse observations. *Astrophys. J.* **895**, 123.

Boe, B., Habbal, S., Druckmüller, M., Ding, A., Hodérova, J., Starha, P.: 2020, CME-induced thermodynamic changes in the corona as inferred from Fe XI and Fe XIV emission observations during the 2017 August 21 total solar eclipse. *Astrophys. J.* **888**, 100. DOI.

Caspi, A., Seaton, D.B., Tsang, C., DeForest, C., Bryans, P., Samra, J., DeLuca, E., Tomczyk, S., Burkepile, J., Gallagher, P., Golub, L., Judge, P.G., Laurent, G.T., West, M., Zhukov, A.: 2019, Novel observations of the middle corona during the 2017 total solar eclipse. In: *AGU Fall Meeting Abs.* **2019**, SH13A.

Chen, Y., Tian, H., Su, Y., Qu, Z.: 2018, Diagnosing the magnetic field structure of a coronal cavity observed during the 2017 total solar eclipse. *Astrophys. J.* **218**, 856. DOI. ADS.

Dani, T., Priyatikanto, R., Rachman, A.: 2016, Ludendorff coronal flattening index of the total solar eclipse on March 9, 2016. In: *Internat. Symp. Sun, Earth, Life*, *J. Phys.* **CS-771**, 012005. DOI.

Druckmüller, M., Rušin, V., Minarovjech, M., Saniga, M.: 2006, *Contrib. Astron. Obs. Skaln. Pleso* **36**, 31.

Filippov, B.P., Koutchmy, S., Lefaudeux, N.: 2020, *Solar Phys.* **295**, 24. DOI.

Golub, L., Pasachoff, J.: 2010, *The Solar Corona*, Cambridge University Press, Cambridge. ISBN 9781139629003. DOI.

Golub, L., Pasachoff, J.M.: 2017, *The Sun*, Reaktion, London.

Habbal, S.R., Druckmüller, M., Alzate, N., Ding, A., Johnson, J., Starha, P., Hoderova, J., Boe, B., Constantinou, S., Arndt, M.: 2021, Identifying the coronal source regions of solar wind streams from total solar eclipse observations and in situ measurements extending over a solar cycle. *Astrophys. J. Lett.* **911**, L4. DOI.

Hanaoka, Y., Hasuo, R., Hirose, T., Ikeda, A.C., Ishibashi, T., Manago, Yukio Masuda, Y., Morita, S., Nakazawa, J., Ohgoe, O., Sakai, Y., Sasaki, K., Takahashi, K., Toi, T.: 2018, Solar coronal jets extending to high altitudes observed during the 2017 August 21 total eclipse. *Astrophys. J.* **860**, 142.

Hudson, H.S., Peticolas, L., Johnson, C., White, V., Bender, M., Collier, B., Guevara Gomez, J.C., Koh, J., Konerding, D., Martínez Oliveros, J.C., McIntosh, S., Kruse, B., Mendez, B., Pasachoff, J., Ruderman, I., Zevin, D.: 2021, The eclipse megamovie project. *J. Astron. Hist. Herit.* **24**(4), 1080. ADS.

Judge, P., Berkey, B., Boll, A., Bryans, P., Burkepile, J., Cheimets, P., DeLuca, E., de Toma, G., Gibson, K., Golub, L., Hannigan, J., Madsen, C., Marquez, V., Richards, A., Samra, J., Sewell, S., Tomczyk, S., Vera, A.: 2019, Solar eclipse observations from the ground and air from 0.31 to 5.5 microns. *Solar Phys.* **294**, 166. DOI.

Koutchmy, S.: 1988, Small scale coronal structures. In: Altrock, R.C. (ed.) *Solar and Stellar Coronal Structure and Dynamics, Proc. 9th Sac Peak Summer Workshop*, NSO, Sunspot, 208.

Koutchmy, O., Koutchmy, S., Nitschelm, C., Sykora, J., Smartt, R.S.: 1988, Image processing of coronal pictures. In: Altrock, R.C. (ed.) *Solar and Stellar Coronal Structure and Dynamics, Proc. 9th Sac Peak Summer Workshop*, NSO, Sunspot, 256.

Kumar, S., Paul, A., Vaidya, B.: 2020, A comparison study of extrapolation models and empirical relations in forecasting solar wind. *Front. Astron. Space Sci.* **7**, 92. DOI. ADS.

Lamy, P., Gilardy, H., Llebaria, A., Quémerais, E., Ernandes, F.: 2021, LASCO-C3 observations of the K- and F-coronae over 24 years (1996 - 2019): Photopolarimetry and electron density distribution. *Solar Phys.* **296**, 76. DOI.

Liang, Y., Qu, Z.Q., Chen, Y.J., Zhong, Y., Song, Z.M., Li, S.Y.: 2021, Registration and imaging polarimetry of the 6374 Å red coronal line during the 2017 total solar eclipse. *Mon. Not. Roy. Astron. Soc.* **503**, 5715. DOI.

Lockwood, C.A., Pasachoff, J.M., Seaton, D.B., Sliski, D., Lefaudeux, N.: 2020, Compositing eclipse images from the ground and from space. *Res. Notes AAS* **4**, 133.

Ludendorff, H.: 1934, Uber die Abhangigkeit der Form der Sonnenkorona ven der Sonnenfleckenhaufigkeit. *Sitz.ber. Preuss. Akad. Wiss. Phys.-Math. Kl.* **16**, 200.

Madsen, C.A., Samra, J.E., Del Zanna, G., DeLuca, E.E.: 2019a, Coronal plasma characterization via coordinated infrared and extreme ultraviolet observations of a total solar eclipse. *Astrophys. J.* **880**, 102. DOI. ADS.

Madsen, C.A., Samra, J., Tañón Reyes, N., DeLuca, E.: 2019b, The 2019 AIR-spec mission: Results from coordinated infrared and EUV spectroscopic observations of the corona during the South Pacific total solar eclipse. In: *AGU Fall Meeting Abs.* **2019**, SH33A. ADS.

Mikić, Z., Downs, C., Linker, J.A., Caplan, R.M., Mackay, D.H., Upton, L.A., Riley, P., Lionello, R., Török, T., Titov, V.S., Wijaya, J., Druckmüller, M., Pasachoff, J.M., Carlos, W.: 2018, Predicting the corona for the 21 August 2017 total solar eclipse. *Nature Astron.* **2**, 913. DOI.

November, L.J., Koutchmy, S.: 1996, White-light coronal dark threads and density fine structure. *Astrophys. J.* **466**, 512. DOI. ADS.

Pasachoff, J.M.: 2017a, Heliophysics at total solar eclipses. *Nature Astron.* **1**, 0190.

Pasachoff, J.M.: 2017b, The great solar eclipse of 2017. *Sci. Am.* **317**, 54.

Pasachoff, J.M.: 2018, Science at the great American eclipse. *Astron. Geophys.* **59**, 4.1.

Pasachoff, J.M., Fraknoi, A.: 2017, Resource letter OSE-1 on observing solar eclipses. *Am. J. Phys.* **85**, 485. DOI.

Pasachoff, J.M., Rušin, V., Druckmüller, M., Saniga, M.: 2007, Fine structures in the white-light solar corona at the 2006 eclipse. *Astrophys. J.* **665**, 824.

Pasachoff, J.M., Rušin, V., Druckmüller, M., Druckmüllerová, H., Bělík, M., Saniga, M., Minarovjech, M., Marková, E., Babcock, B.A., Souza, S.P., Levitt, J.S.: 2008, Polar plume brightening during the 29 March 2006 total eclipse. *Astrophys. J.* **682**, 638.

Pasachoff, J.M., Rušin, V., Druckmüllerová, H., Saniga, M., Lu, M., Malamut, C., Seaton, D.B., Golub, L., Engell, A.J., Hill, S.W., Lucas, R.: 2011a, Structure and dynamics of the 11 July 2010 eclipse white-light corona. *Astrophys. J.* **734**, 114. DOI.

Pasachoff, J.M., Rušin, V., Saniga, M., Druckmüllerová, H., Babcock, B.A.: 2011b, Structure and dynamics of the 22 July 2009 eclipse white-light corona. *Astrophys. J.* **742**, 29. DOI.

Pasachoff, J.M., Rušin, V., Saniga, M., Babcock, B.A., Lu, M., Davis, A.B., Dantowitz, R., Gaintatzis, P., Seiradakis, J.H., Voulgaris, A., Seaton, D.B., Shiota, K.: 2015, Structure and dynamics of the 13/14 November 2012 white-light corona. *Astrophys. J.* **800**, 90. DOI.

Pasachoff, J.M., Lockwood, C., Meadors, E., Yu, R., Perez, C., Peñaloza-Murillo, M.A., Seaton, D.B., Voulgaris, A., Dantowitz, R., Rušin, V., Economou, T.: 2018, Images and spectra of the 2017 total solar eclipse corona from our Oregon site. *Front. Astron. Space Sci.* **5**, 37. DOI.

Pasachoff, J.M., Lockwood, C.A., Inoue, J.L., Meadors, E.N., Voulgaris, A., Sliski, D., Sliski, A., Reardon, K.P., Seaton, D.B., Caplan, R.M., Downs, C., Linker, J.A., Schneider, G., Rojo, P., Sterling, A.C.: 2020, Early results from the solar-minimum 2019 total solar eclipse. In: Kosovichev, A., Strassmeier, K., Jardine, M. (eds.) *Solar and Stellar Magnetic Fields: Origins and Manifestations*, *IAU Symp.*, **354**, Cambridge University Press, Cambridge, 3. DOI.

Pasachoff, J.M., Downs, C., Linker, J., Caplan, R., Riley, P., Lionello, R., Möller, A., Rušin, V., Vanur, R., Carlos, W.: 2021, Observational validation of predictions for the 2020 eclipse corona, AAS/Solar Physics Div., 229.01. aas238-aas.ipostersessions.com/Default.aspx?s=E0-A8-3C-3E-F5-80-5F-94-8F-2A-0F-F7-31-EF-DC-44.

Pasachoff, J.M., Rušin, V., Davis, A.B., Seaton, D.B., Lockwood, C.: 2022, Intricacies of the 2013 November 3 hybrid-eclipse white-light corona. *Solar Phys.* Submitted.

Peticolas, L., Hudson, H., Johnson, C., Zevin, D., White, V., Oliveros, J.C.M., Ruderman, I., Koh, J., Konerding, D., Bender, M., Cable, C., Kruse, B., Yan, D., Krista, L., Collier, B., Fraknoi, A., Pasachoff, J.M., Filippenko, A.V., Mendez, B., McIntosh, S.W., Filippenko, N.L.: 2019, Eclipse megamovie 2017 successes and potential for future work. In: Buxner, S.R., Shore, L., Jensen, J.B. (eds.) *Celebrating the 2017 Great American Eclipse: Lessons Learned from the Path of Totality* **CS-516**, Astron. Soc. Pacific, San Francisco, 337.

Pishkalo, M.I.: 2011, Flattening index of the solar corona and the solar cycle. *Solar Phys.* **270**, 347. DOI.

Rušin, V.: 2000, Shape and structure of the white-light corona over solar cycles. In: Livingston, W., Ozguc, A. (eds.) *The Last Total Solar Eclipse of the Millennium* **CS-205**, Astron. Soc. Pacific, San Francisco, 17. ADS.

Rušin, V.: 2017, The flattening index of the eclipse white-light corona and magnetic fields. *Solar Phys.* **292**, 24. DOI.

Samra, J.E., Judge, P.G., DeLuca, E.E., Hannigan, J.W.: 2018, Discovery of new coronal lines at 2.843 and 2.853 μm. *Astrophys. J. Lett.* **856**, L29. DOI.

Seaton, D.B., Darnel, J.M., Hsu, V., Hughes, J.M.: 2020, GOES-R series solar dynamics. In: Goodman, S.J., Schmit, T.J., Daniels, J., Redmon, R.J. (eds.) *The GOES-R Series*, Elsevier, Amsterdam, 219. DOI. Chapter 18.

Stellmacher, G., Koutchmy, S., Lebecq, C.: 1986, The 1981 total solar eclipse. III - Photometric study of the prominence remnant in the reversing South polar field. *Astron. Astrophys.* **162**, 307.

Svalgaard, L., Cliver, E.W., Yohsuke, K.: 2005, Sunspot cycle 24: Smallest cycle in 100 years? *Geophys. Res. Lett.* **32**, L01104. DOI.

Wang, Y.-M., Sheeley, N.R. Jr., Rich, N.B.: 2007, Coronal pseudostreamers. *Astrophys. J.* **658**, 1340. DOI. ADS.

Williams, L., Caspi, A., Seaton, D., Samra, J.: 2020, Comparisons of novel imaging and spectroscopic infrared eclipse observations in 2017. In: *AAS/Solar Physics Div. Meet.*, *Bull. Am. Astron. Soc.* **52**, 210.12.

Zirker, J.B., Koutchmy, S., Nitschelm, C., Stellmacher, G., Zimmermann, J.P., Martinez, P., Kim, I., Dzyubenko, N., Kurochka, L., Makarov, V.: 1992, Structural changes in the solar corona during the July 1991 eclipse. *Astron. Astrophys.* **258**, L1.